Microtomography to Study Flame Retardants, Coronary Arteries, Volcanic Glasses, and the Structure of the Eye

L.G. Butler,[1] K. Ham,[2] H. Jin,[3] R.L. Kurtz,[4] M. Rivers[5]

[1]Department of Chemistry and [2]Center for Advanced Microstructures & Devices (CAMD),
Louisiana State University (LSU), Baton Rouge, LA, U.S.A.
[3]Department of Materials Science and Engineering, Northwestern University, Evanston, IL, U.S.A.
[4]Department of Physics and Astronomy, LSU, Baton Rouge, LA, U.S.A.
[5]Consortium for Advanced Radiation Sources (CARS), The University of Chicago, Chicago, IL, U.S.A.

Introduction

Tomography is one of the best nondestructive tools for conducting studies of the internal structure of objects as well as elemental studies of objects. For example, consider a concentration or distribution map in 3-D of a material. Consider calcification attached to arterial walls; new calcification can develop within a few years after a heart bypass operation. Making images of an eyeball is a challenge for the nondestructive technique of synchrotron tomography with high resolution. It has the potential to reveal drainage channels and optic nerves in 3-D. These samples and more were imaged at the GEOCARS beamline at the APS, and ideas were shared about tomography data acquisition and analysis.

Methods and Materials
Flame Retardants

There are three issues related to brominated aromatic flame retardants that need to be addressed. First, the solubility of a brominated aromatic with high-impact polystyrene (HIPS) varies with its molecular structure. Good miscibility is desired, or else the stability of the final product can be poor. Second, brominated aromatics are difficult to observe with some of the more common spectroscopic methods typically used for polymer blend characterization. For example, solid-state ^{13}C nuclear magnetic resonance (NMR) is a common spectroscopic method for polymer studies, yet the quadrupolar bromine nucleus causes such line broadening of the ^{13}C resonances that miscibility is difficult to ascertain from the spectrum; hence, the relatively uncommon technique of ^{81}BR nuclear quadrupole resonance (NQR) is used [1]. Third, there is some concern about the bioaccumulation of brominated aromatics, especially phenolic degradation products of perbrominated biphenyl ethers, and their subsequent role as estrogen mimics [2]. Commercial brominated flame retardants (Fig. 1) have different solubilies in HIPS. An aromatic ether — 1-(2,3,4,5,6-pentabromophenoxy)-2,3,4,5,6-pentabromobenzene

(Saytex 102) — is miscible in HIPS. However, a somewhat larger molecule — 3,3',4,4',5,5',6,6'-octabromo-N,N'-ethylenediphthalimide (Saytex BT-93) — appears to exist as microcrystalline domains dispersed in HIPS. Although, NMR imaging could, in principle, be used to study miscibility, we consider synchrotron radiation microtomography to be a faster and more informative technique. Tomography data sets were acquired at seven different x-ray energies, including energies both above and below the Br K edge and the Sb K edge.
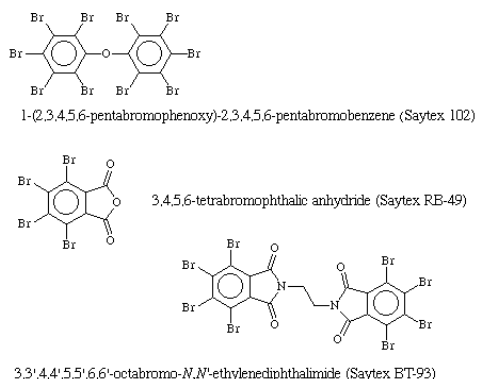

FIG. 1. Brominated aromatic flame retardants.

Atherosclerosis

Human atherosclerotic arteries removed from three white males aged 51, 55, and 70 were measured. The arteries were obtained from the Pathology Department of the LSU Medical Center in New Orleans. Two kinds of arteries, native and bypass, were used in this study, and images were taken at two different heights for each native artery. Figure 2 is a schematic drawing of a native artery and bypass. The native arteries were present since birth. The bypass arteries were inserted during heart bypass surgery. The bypasses were removed because they had filled up again with plaque. The native arteries of the A and B specimens were from the left circumflex; the C sample was from the anterior

descending coronary artery. Each artery was cut to a length of about 20 mm and inserted longitudinally into a plastic straw; each sample was packed in a separate straw. Each straw was sealed at the bottom and top to prevent dehydration. The arteries were kept frozen prior to the tomographic measurements. Experiments were done after the arteries thawed.
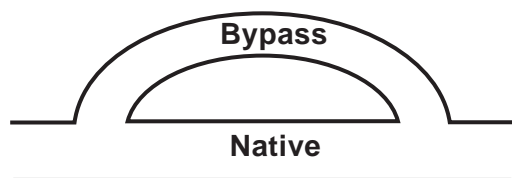

FIG. 2. Schematic drawing of a native artery and bypass.

Volcanic Glasses

About 15-million-year-old Columbia River basalt glasses were imaged, with an emphasis on cracks and porosity. The stereometric analysis of phase proportions/percentages and phase size distributions will provide data on a crack network at a resolution sufficient to exploit the algorithms for lamination analysis that can be adapted to crack network analysis. Also, mass balance calculations comparing chemistry to proportions will provide useful information on the synthetic glass and materials/environmental science connection.

Eyeballs

Eyeballs of dogs and rats were imaged in different environments. A monkey's scleral shell in saline solution was imaged at 30 keV.

Results
Flame Retardants

The multiple 3-D images were converted to a single 3-D map of flame retardant distribution by a voxel-by-voxel nonlinear least square fit of x-ray absorption. The absorptions of the pure phases, flame retardants and HIPS, were calculated from a National Institute of Standards and Technology (NIST) database, and the least square fit routine was constrained to return physically reasonable flame retardant concentrations for each voxel. The 3-D flame retardant image (Fig. 3) shows the concentration map of only BT93 and Sb_2O_3. The average concentration for BT93 was 3.781 vol% (cf. 4.250% by chemical analysis) and that for Sb_2O_3 was 0.597 vol% (cf. 0.714%). The map also clearly shows an inhomogeneous distribution of BT-93 and Sb_2O_3, the least soluble flame retardant. But higher concentrations (>5.36 vol% for BT93, >1.19 vol% for

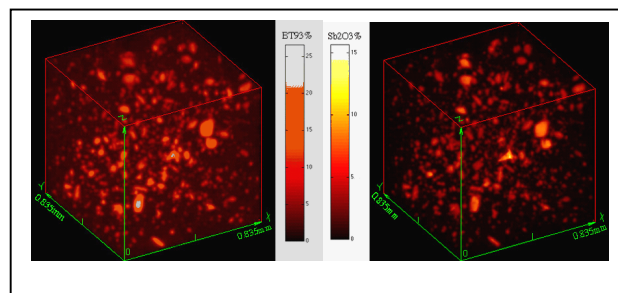Sb_2O_3) are only 5.2% of voxels. A particle size analysis has been done [3].

FIG. 3. 3-D flame retardant image of only BT93 and Sb_2O_3.

Atherosclerosis

Three types of plaque components were distinguished by their brightness in these samples, indicating the low, medium, and high mass densities previously indicated by other clinical imaging methods. The low-density component was identified as lipid-rich deposits (fatty plaque), the medium density as fibrous plaque, and the high mass density as calcified plaque [4, 5]. These three phases were observed in the absorption profile, as shown in Fig. 4. The absortion coefficient of fibrous plaque of 12.5-keV x-rays is about 2.28 cm^{-1} (twice that of fatty plaque). The calcium deposit has around 10 times higher absorption than the fibrous plaque. The cross-sectional images of the native arteries clearly show the 3-D morphologies and distributions of the plaque components in atherosclerotic arteries (Fig. 5). Some calcified plaques were separately distributed as small clusters, while some were large continuous pieces along the vessel axis. The density of the calcification edges was larger than that of the interiors, which is also shown in Fig. 4.
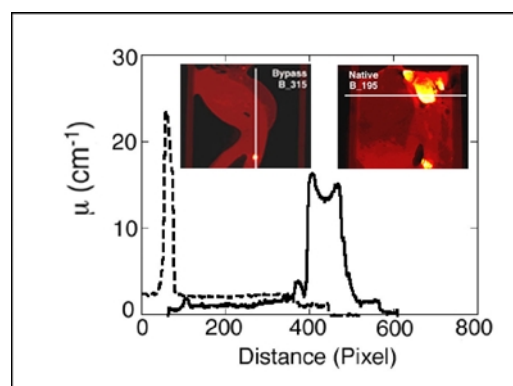

FIG. 4. Absorption along the bypass (dashed line) and native (solid line) ateries of a 55-yr old male. These lines span all three plaque phases and air.

The volume fraction of calcification was determined by thresholding the absorption of calcification and air to estimate volumes of calcified plaques and artery walls. The volume ratios of calcification to artery wall for the three native samples were 3.7 ±0.2%, 6.0 ±1.3%, and 20 ±3%, respectively, while the ratios for the bypass specimens were only 0.025 ±0.004%, 0.032 ±0.007%, and 0.021 ±0.002%, respectively, orders of magnitude lower than the ratios for the native ones [6].
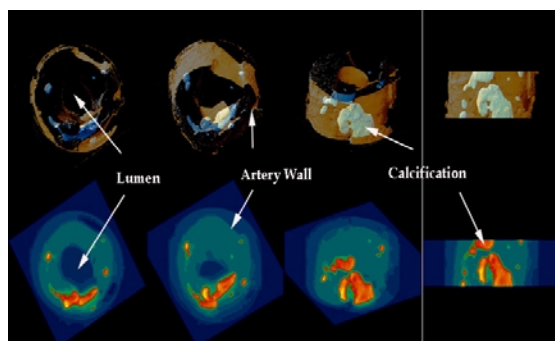

FIG. 5. 3-D view of portion of native artery at different angles. Lumen, artery wall, and calcifications are indicated.

Volcanic Glasses

Eight different volcanic glasses were imaged with 40-keV x-rays. Results showed three different phases: glass, olivine, and plagioclase (Fig. 6). Figure 7 shows the 3-D view of crack channels in volcanic glass.
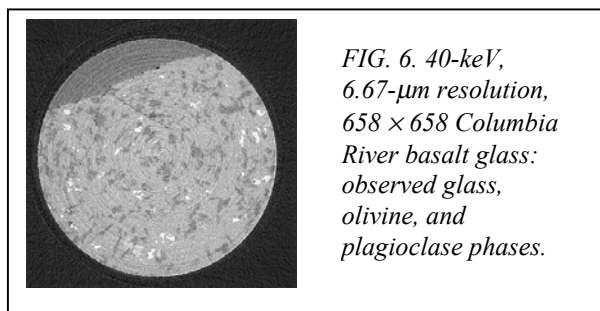

FIG. 6. 40-keV, 6.67-μm resolution, 658 × 658 Columbia River basalt glass: observed glass, olivine, and plagioclase phases.
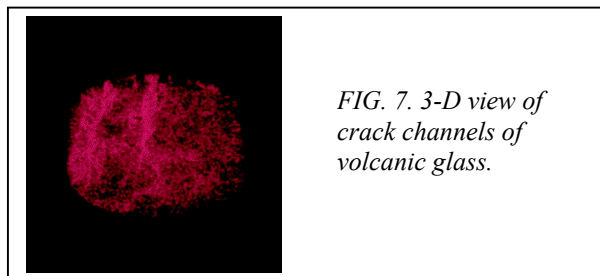

FIG. 7. 3-D view of crack channels of volcanic glass.

Eyeballs

Without a contrast agent, the inner soft tissues in the eyeball were hardly discernible. Because of the size of the eyeball, several horizontal images were taken to stitch for a larger field of view with high resolution. Optic nerve images indicated nerve bundles with 5.67-μm resolution.

Discussion

Synchrotoron x-ray tomography is a very useful tool for providing 3-D internal views at micrometer order resolution. Also, 3-D chemical analysis at near micrometer resolution is demonstrated with multiple data sets acquired by synchrotron x-ray tomography.

Acknowledgments

References

[1] A.A. Mrse, Y. Lee, P.L. Bryant, F.R. Fronczek, L.G. Butler, and L.S. Simeral, Chem. Mater. **10**, 1291-1300 (1998).
[2] K.S. Betts, Environ. Sci. Technol. **35**, 274A-275A (2001).
[3] K. Ham et al., Chem. Mater. (submitted 2003).
[4] R.A. Vogel, Am. J. Cardiac Imaging **2,** 110-115 (1988).
[5] S. Vallabhajosula and V. Fuster, J. Nucl. Med. **38,** 1788-1796 (1997).
[6] H. Jin et al., Phys. Med. Biol. **47**, 4345-4356 (2002).